

# Redox Features of CuO/CeO<sub>2</sub> Catalysts in the Preferential Oxidation of CO

Enrique Rodríguez Castellón<sup>1</sup>, Álvaro Reyes Carmona<sup>1</sup>, Ana Arango Díaz<sup>1</sup>, Antonio Jiménez-López<sup>1</sup>,  
Elisa Moretti<sup>2</sup>, Loretta Storaro<sup>2</sup>, Aldo Talon<sup>2</sup>, Maurizio Lenarda<sup>2</sup>

1. Departamento de Química Inorgánica, Cristalografía y Mineralogía (Unidad Asociada al ICP-CSIC), Facultad de Ciencias, Universidad de Málaga, Campus de Teatinos, E-29071 Málaga, Spain. [castellon@uma.es](mailto:castellon@uma.es)

2 Dipartimento di Chimica, Università Ca' Foscari di Venezia, Via Torino 155/B, 30172 Venezia, Italy.

## 1. Introduction

The reforming of methanol or ethanol is considered to be a feasible method to produce hydrogen-rich gas streams as feed for proton-exchange membrane fuel cells (PEMFCs). Nevertheless, CO is a typical by-product of the process that must be reduced down to ppm levels in order to become suitable to be used as feed. The selective oxidation of CO (CO-PROX) is considered one of the most straightforward and cost effective methods to achieve the required low levels of CO. Catalysts based on the CuO-CeO<sub>2</sub> couple are highly active and selective in CO-PROX process, but also from an economical point of view. The performances of these catalysts in CO-PROX appear to be related to the peculiar synergistic redox properties in the presence of copper-ceria interfacial sites. The CO-PROX activity and selectivity appears to be improved by the presence of highly dispersed copper species on the ceria surface that favor the formation of oxygen vacancies at the copper-ceria boundaries improving copper reducibility. The presence of ZrO<sub>2</sub> in this system improves the oxygen-storage capacity due to the formation of Ce<sub>x</sub>Zr<sub>1-x</sub>O<sub>2</sub>, mixed oxide modifying the redox properties and thermal resistance of the catalysts. The combination of hydrogen temperature programmed reduction (H<sub>2</sub>-TPR) and XPS measurements are two powerful tools to study the redox features of these solids in the CO-PROX process. Catalysts based on Zr doped mesoporous silica of type SBA-15 will be studied by H<sub>2</sub>-TPR and XPS in order to explain their catalytic performance in the CO-PROX process.

The Zr containing supports based on SBA-15 were synthesized following the method of Zajac et al. [1], using a Si/Zr ratio of 10, 20 and infinite (without Zr added). The materials obtained were labelled as SBAZr10, SBAZr20 and SBA, respectively. The mesoporous solids were impregnated via incipient wetness method using aqueous solutions of copper(II) and cerium(III) salts. The catalysts were prepared with a fixed cerium loading of 20 wt.% and loadings of copper (3, 6 and 12 wt.%). The samples were dried 12 h at 60°C and then calcined at 450°C for 4 h. The catalysts were labelled as SBAZr<sub>y</sub>Ce<sub>20</sub>Cu<sub>x</sub>, where x denotes the weight percentage of copper and y the Si/Zr ratio.

H<sub>2</sub>-TPR experiments were carried with ~ 0.1 g of freshly calcined catalyst that was placed on top of wool glass in a quartz reactor. In order to remove contaminants, the powder was pre-treated in helium (20 cm<sup>3</sup> min<sup>-1</sup>) to 350°C for 1 h. After cooling to ambient temperature, TPR experiments were carried out in 10 vol.% H<sub>2</sub>/Ar (30 cm<sup>3</sup> min<sup>-1</sup>) increasing the temperature from 40°C to 800°C (10°C min<sup>-1</sup>), by a temperature programmable controller. XPS were collected using a PHI 5700 spectrometer with non monochromatic Mg K $\alpha$  radiation (300W, 15 kV, 1253.6 eV) for the analysis of the core level signals of O 1s, Si 2p, Zr 3d, Ce 3d and Cu 2p. A short acquisition time of 10 min was used to examine C 1s and Cu 2p XPS regions in order to avoid, as much as possible, photoreduction of Cu<sup>2+</sup> species.

All the samples resulted active and selective in the CO-PROX in the 40-190°C temperature range, and the in Fig 1 are shown as an example the catalytic performance of the materials supported on SBAZr10 with three different Cu loadings. The content of Cu affects to the catalytic performance, especially at low reaction temperature. At 115 °C the conversion % is close 100% for the catalysts with 6 or 12wt% of Cu. More interestingly, the selectivity to CO<sub>2</sub> is 100% at low temperature without taking place the oxidation of H<sub>2</sub>, being the sample with a 6 wt% of Cu the best one. Other catalysts supported on SBAZr 20 and SBA exhibit poorer catalytic performances than those supported on SBAZr10.

XPS was used to obtain information about the valence/oxidation state of the elements and surface composition of the active metals by inspecting the spectral line shape and the intensities of the Ce 3d and Cu 2p core-level electrons. The samples were analyzed before and after a CO-PROX catalytic test. The reduction degree of ceria was calculated by considering the relative intensity of the  $u_0$  ( $v_0$ ) and  $u'$  ( $v'$ ) peaks to the intensity of Ce 3d region. The core level spectrum Cu 2p of the solids before catalysis show a main Cu 2p<sub>3/2</sub> peak that can be decomposed in two contributions at 932.6 eV and 934.8 eV. These two contribution are ascribed to the presence of CuO particles (contribution at 934.8 eV) and reduced copper species or small clusters of copper

(contribution at 932.6 eV) formed by the strong interaction between copper and ceria. After reaction, the relative intensity of the contribution due to CuO at 934.8 eV decreases (see Figure 13), and the  $Cu_{red}/CuO$  increases.  $H_2$ -TPR results indicated that samples with Cu species with lower reduction temperature exhibit a much better catalytic performance as shown in Figure 2.

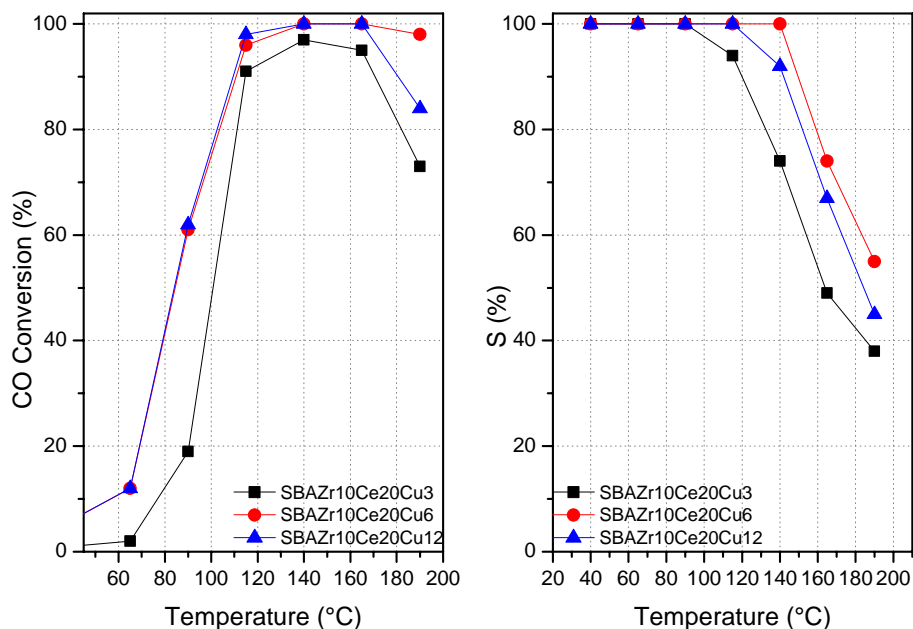


**Figure 1.-** Variation of the a CO conversion and b selectivity towards to  $CO_2$  as a function of the reaction temperature obtained for the catalysts SBAZr10 with 20 wt% of Ce and 3, 6 and 12 wt% of Cu. Operating conditions:  $k = 2$ ;  $W/F = 0.18 \text{ g s cm}^{-3}$ ; 1.2% CO, 1.2%  $O_2$ , 50%  $H_2$ , He balance (vol.%).

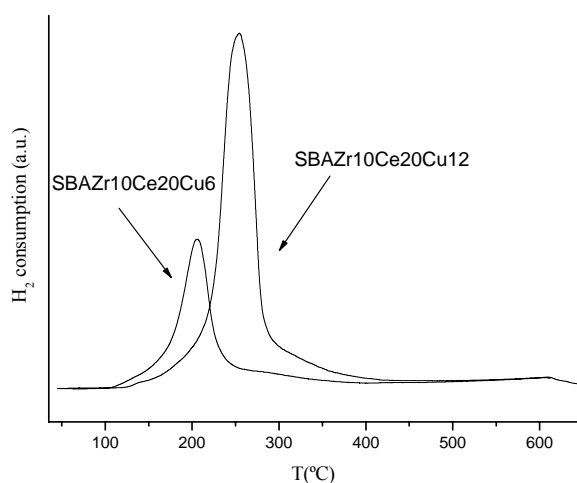


**Figure 2.**  $H_2$ -TPR curves for catalysts SBAZr10Ce20Cu6 and SBAZr10Ce20Cu12

### Acknowledgements

The Ministero dell'Università e Ricerca (MiUR-PRIN 2006) is gratefully acknowledged for financial support by the Italian authors. The Spanish authors thank the Project MAT09-10481 (Ministerio de Ciencia e Innovación).

### References

- [1] K. Szczodrowski, B. Prélot, S. Lantenois, J. Zajac, M. Lindheimer, D. Jones, A. Julbe, A. van der Lee. *Microporous and Mesoporous Materials* **110**, 111–118 (2008).
- [2] X. Tang, B. Zhang, Y. Li, Y. Xu, Q. Xin, W. Shen, *Appl. Catal. A* **288**, 116-121 (2005).